GEOCHEMISTRY

Carbon recycling efficiency and phosphate turnover by marine nitrifying archaea

Travis B. Meador[1]*[†], Niels Schoffelen[2], Timothy G. Ferdelman[2], Osmond Rebello[1,2], Alexander Khachikyan[2], Martin Könneke[1]

Thaumarchaeotal nitrifiers are among the most abundant organisms in the ocean, but still unknown is the carbon (C) yield from nitrification and the coupling of these fluxes to phosphorus (P) turnover and release of metabolites from the cell. Using a dual radiotracer approach, we found that *Nitrosopumilus maritimus* fixed roughly 0.3 mol C, assimilated 2 mmol P, and released ca. 10^{-2} mol C and 10^{-5} mol P as dissolved organics (DOC and DOP) per mole ammonia respired. Phosphate turnover may influence assimilation fluxes by nitrifiers in the euphotic zone, which parallel those of the dark ocean. Collectively, marine nitrifiers assimilate up to 2 Pg C year^{-1} and 0.05 Pg P year^{-1} and thereby recycle roughly 5% of mineralized C and P into marine biomass. Release of roughly 50 Tg DOC and 0.2 Tg DOP by thaumarchaea each year represents a small but fresh input of reduced substrates throughout the ocean.

INTRODUCTION

In the deep dark ocean, widely distributed ammonia-oxidizing Thaumarchaeota (*1*) fix C at rates that parallel riverine transport of organic matter to the ocean or C buried in marine sediments [e.g., (*2*)]. As revealed by culture studies of the thaumarchaeon *Nitrosopumilus maritimus*, this important flux of the global C budget is supported by the high affinity of this microbe for ammonia (*3*) and its efficient C fixation pathway (*4*). Ship-board radiotracer incubations of bathypelagic microbes suggest that dark ocean chemoautotrophy ranges from 0.8 to 1.2 Pg C year^{-1} (*2*, *5*, *6*), but these estimates are >100% higher than geochemical mass balance estimates, which range up to 0.4 Pg C year^{-1} (*7*) and have assumed (i) complete oxidation of organic nitrogen (N) sinking below the euphotic zone and (ii) a C yield from nitrification of 10% [$C_0/N_n = 0.1$; *Nitrosomonas marina*; (*8*, *9*)]. This discrepancy has been explained by missing transport of reduced N into the bathypelagic or alternative energy sources to support dark ocean chemoautotrophy (*2*, *6*, *7*, *10*). However, in theory, C fixation by the 3-hydroxypropionate/4-hydroxybutyrate (HP/HB) pathway should lower the adenonine 5′-triphosphate (ATP) demand of thaumarchaea (*4*) and thus translate to a higher C yield for archaeal nitrification. This important coupling, which would adjust the ranking of marine nitrification in the global C budget, has not yet been established by empirical evidence.

Thaumarchaea may be relatively more abundant than other microbes in the deep ocean, but absolute cell densities of marine archaea are actually the highest in the surface ocean (*1*, *11*), owing in part to their strong affinity for ammonia (*3*). By assuming a conservative, median value for specific nitrification rates in surface waters, previous reports have suggested that epipelagic thaumarchaea may access 43% of ammonia and contribute roughly half of the flux of "new nitrate" upwelled from the subsurface, with substantial consequences for estimates of new versus recycled production and the export of organic material to depth (*2*, *12*). Furthermore, C fixation by chemo-autotrophs in the surface ocean may be twice that of the deep sea (*2*).

This flux may be controlled, however, by competition for nutrients, such as dissolved inorganic phosphorus (P_i), the availability of which is known to limit biological production in open ocean gyres where recycled production is dominant (*13*, *14*). While the small biovolume (*15*) and high-affinity phosphate and phosphonate transporters encoded in the genome (*16*) should allow for thaumarchaea to compete for scarce amounts of P_i in the surface ocean, the effect of P limitation on archaeal nitrification and the C yield from nitrification remains unknown. Despite the important roles of archaea in marine nitrification (*15*, *17*), C fixation (*5*, *18*, *19*), and the release of labile metabolites that may fuel the microbial loop (*20*), the coupling of archaeal ammonia oxidation to marine nutrient fluxes is still poorly understood.

This study sought to improve our understanding of thaumarchaeal contributions to marine nutrient recycling and to identify the responses of thaumarchaea to P limitation by determining cellular budgets and the coupled fluxes of C, N, and P by two cultured strains of *N. maritimus*. These aims were achieved via radiotracer experiments that quantified cell-specific uptake rates of C and P as well as dissolved organic phosphorus and carbon (DOP and DOC) production rates of *N. maritimus* growing under a range of P_i concentrations. The P acquisition adaptations of *N. maritimus* isolated from a saltwater aquarium [strain *SCM1*; (*15*)] were further compared to those of a closely related environmental strain, *N. maritimus NAOA6* (*21*), isolated from surface waters of the Benguela upwelling system at station GeoB12806 (13.6°C; 25°S, 14°23′E; R/V Meteor cruise M76/1).

RESULTS

AOA growth response to P limitation

N. maritimus SCM1 grown in synthetic Crenarchaeota medium (SCM) with P_i as low as 0.4 µM reached cell densities of 10^8 cells ml^{-1} (fig. S1, A and B), which is in the range for growth in SCM medium that contains ca. 30-fold higher P_i (14.7 µM; *4*). However, the maximum cell density was reduced by at least 10-fold in SCM medium amended with <0.2 µM P_i, with growth of environmental strain *N. maritimus NAOA6* being more negatively affected than aquarium strain *SCM1* (fig. S1, A and B). Provided with an ample energy source (i.e., 1 mmol liter^{-1} ammonium), nitrite was continuously evolved by *N. maritimus* grown in medium with initial P_i > 0.4 µM (hereafter P-replete medium >0.4 µM P_i > P-deplete medium).

[1]MARUM Center for Marine Environmental Sciences and Dept. of Geosciences, University of Bremen, Bremen, Germany. [2]Department of Biogeochemistry, Max Planck Institute for Marine Microbiology, Bremen, Germany.
*Corresponding author. Email: travis.meador@bc.cas.cz
†Present address: Biology Center Czech Academy of Sciences, Soil & Water Research Infrastructure, Na Sádkách 7, 370 05 České Budějovice, Czechia.

Nitrite production plateaued at 0.25 mM in experiments initiated at $P_i < 0.2$ µM P_i (fig. S1, C and D) but nevertheless exhibited a period of linear increase at rates ranging from 0.3 to 5 µmol NO_2 liter^{-1} hour^{-1} (table S1 and fig. S3).

Linear increases in ^{14}C and ^{33}P uptake by *N. maritimus* coincided with the exponential growth phase, with the exceptions of experiments performed in P-deplete media, which exhibited first-order uptake of C and P (table S1 and fig. S3) despite little evidence of growth (i.e., cell densities remained static and below 10^7 ml^{-1}; fig. S1 and see Materials and Methods). Absolute C fixation rates were comparable between the two strains, approaching 1.5 µmol C liter^{-1} hour^{-1} under P-replete conditions and dropping to roughly 0.35 µmol C liter^{-1} hour^{-1} in experiments where no KH_2PO_4 was added to the medium and growth was limited (table S1 and fig. S3). When grown under P-deplete conditions, P uptake by *N. maritimus NAOA6* (5 nmol P liter^{-1} hour^{-1}) was roughly fivefold faster than that of *SCM1* (1 nmol P liter^{-1} hour^{-1}; table S1 and fig. S3).

Coupled rates of C fixation, P_i uptake, and nitrification

Cell-specific rates of both C and P uptake by *N. maritimus NAOA6* were higher for P-limited cells and spanned much larger ranges [1×10^{-18} to 650×10^{-18} mol (amol) C cell^{-1} hour^{-1} and 50×10^{-21} to 2600×10^{-21} mol (zmol) P cell^{-1} hour^{-1}] than strain *SCM1* (5 to 50 amol C cell^{-1} hour^{-1} and 10 to 270 zmol P cell^{-1} hour^{-1}); however, the ratio of C and P assimilation fluxes (C:P_{assim}) by the environmental strain *NAOA6* was more stable (60 to 150) than the aquarium strain *SCM1* (120 to 1000; Fig. 1A). Notably, for *N. maritimus SCM1*, the fastest cell-specific rates of P_i uptake (ca. 210 to 270 zmol P cell^{-1} hour^{-1}) and the lowest C:P_{assim} (120 to 200) were determined for P-limited cells (Fig. 1A). During periods of linear uptake of both C and P (table S1 and fig. S3), cell-specific nitrification rates ranged from 0.1 to 1 fmol NO_2 cell^{-1} hour^{-1} (Fig. 1B). Volumetric nitrification rates were correlated with both volumetric C fixation rate ($R^2 = 0.91$ and 0.94, $P < 0.02$ and 0.01 for strains *SCM1* and *NAOA6*, respectively; Fig. 2A) and P uptake rate ($R^2 = 0.97$ and 0.99, $P < 0.01$ for strains *SCM1* and *NAOA6*, respectively; Fig. 2B). The slopes of these relationships reveal the C and P yields from nitrification ($C_0/N_n = 0.57 \pm 0.09$ and 0.30 ± 0.04 mol mol^{-1}; $P_0/N_n = 1.6 \pm 0.1$ and 2.7 ± 0.1 mmol mol^{-1} for strains SCM1 and *NAOA6*, respectively). However, these slopes integrate potentially distinct trends among P-limited versus P-replete cells. For the aquarium strain *SCM1*, C_0/N_n values ranged from 0.44 to 1.2 (Table 1) and increased linearly with decreasing nitrification rate (fig. S4). C_0/N_n values of the environmental strain *NAOA6* were lower (0.18 to 0.41; Table 1) and showed no trend with volumetric nitrification rate but were rather lowest in incubations where cell-specific nitrification rate increased by an order of magnitude, i.e., for cells with the highest energy demand (fig. S4).

AOA cellular C, N, and P inventory

Cells harvested from the batch cultures prepared for P inventory experiments reached a cell density of 10^6 cells ml^{-1} (fig. S1); P_i was completely consumed in P-deplete medium (initial $P_i \approx 0.35$ µM), and 60 to 85% of P_i was consumed in P-replete cultures (initial $P_i \approx 1.6$ µM; table S2). Cellular P quotas of *N. maritimus NAOA6* were 1.5 ± 0.6 and 0.53 ± 0.20 fg P cell^{-1} for cells grown in P-replete or P-deplete medium, respectively, as determined on the basis of cell counts and measurements of P_i and DOP in growth medium and total P of concentrated biomass (Table 2). C:P and N:P molar ratios

determined via scanning electron microscopy with energy-dispersive spectroscopy (SEM-EDS) measurements of the same concentrated *N. maritimus NAOA6* biomass were 57.7 ± 2.5 and 9.5 ± 1.2, respectively, for cells grown in P-replete media and contained relatively less P (80C:14N:1P) than cells grown in P-deplete medium (Table 2 and table S2) (*22*), which is consistent with the response of bacterioplankton to P limitation (*23*). On the basis of the quantitative, colorimetric determination of cellular P quotas, and the C:N:P ratios determined via SEM-EDS, we calculate C and N cell quotas of 34 ± 14 fg C cell^{-1} and 6.5 ± 2.8 fg N cell^{-1} for *N. maritimus NOAO6* grown in P-replete medium, and 17 ± 6 fg C cell^{-1} and 3.4 ± 1.3 fg N cell^{-1} in P-deplete medium (Table 2).

Phosphate turnover time and specific affinity

P_i turnover was generally slow in P-replete media (τ_{PO4} up to 1000 hours) and very rapid in medium with no P_i amendment (τ_{PO4} as low as 3 hours; Fig. 3). τ_{PO4} was fastest in *NAOA6* experiments but was always >50 hours in experiments with aquarium strain *SCM1*, even when grown in P-deplete medium. There was no growth of *N. maritimus NAOA6* as τ_{PO4} fell below 5 hours in P-starved medium (i.e., with no KH_2PO_4 amendment; fig. S1), but cells exhibited a roughly 20-fold increase in nitrification rates and 500-fold increase in specific affinity for P_i (α°_{PO4}) than those grown under P-replete conditions (Fig. 3, A and B). The α°_{PO4} of *N. maritimus* generally increased in P-deplete media, climbing to $>10^3$ liter g_{cell}^{-1} hour^{-1} (or 10^{-3} liter nmol P^{-1} hour^{-1}) for strain *NAOA6* grown in medium with no KH_2PO_4 amendment, but remained $<10^2$ liter g_{cell}^{-1} hour^{-1} (or 10^{-4} liter nmol P^{-1} hour^{-1}) for aquarium strain *SCM1* (Fig. 3B).

Release of DOC and DOP

DOP in *N. maritimus* large batch cultures increased to 10 to 40 nM by stationary phase and accounted for 2 to 7% of assimilated P_i (table S2). DOP and DOC production by *N. maritimus* was also observed in the radiolabeled fractions. That is, after filtration of radiolabeled cells and precipitation of $^{33}P_i$ or sparging of $H^{14}CO_3^-$, ^{33}P and ^{14}C activity was still detected in the medium, presumably as dissolved organics (i.e., $^{33}A_{DOP}$ and $^{14}A_{DOC}$). On the basis of the $^{33}A_{DOP}$ signal, which was always significantly higher in live treatments than in the respective blank and killed controls ($P < 0.05$), DOP in culture media accounted for 0.5 to 3% of P_i assimilated into *N. maritimus* biomass (table S3). The integrated rates of DOP release, based on our single time point measurement and the maximum cell density, ranged from 5 to 80 zmol P cell^{-1} day^{-1} and were higher under P-deplete conditions for the environmental strain *NAOA6*. DOP release by *N. maritimus SCM1* ranged from 5 to 27 zmol P cell^{-1} day^{-1} (table S3). DOC release was determined only in radiotracer incubations and amounted to roughly 5% of C fixed by *N. maritimus NAOA6* grown in P-replete medium; in contrast, 9 to 19% of C fixed by aquarium strain *SCM1* was released as DOC on average. DOC production ranged from 5 to 55 amol C cell^{-1} day^{-1}, with higher rates observed for strain *SCM1* than *NAOA6* (table S3). These rates are roughly equivalent to the release of up to 0.3 and 3% of the cellular P and C quotas, respectively. The C:P of dissolved organic matter (DOM) produced by *N. maritimus* ranged from 2×10^3 to 8×10^3 for the aquarium strain *SCM1* and was much higher than that of the environmental strain *NAOA6* ($600 < $ C:$P_{DOM} < 900$). Normalized to rates of nitrification, DOP yield (DOP_0/N_n) and DOC yield (DOC_0/N_n) were on the order of 10 µmol mol^{-1} and 50 mmol mol^{-1}, respectively (Table 1).
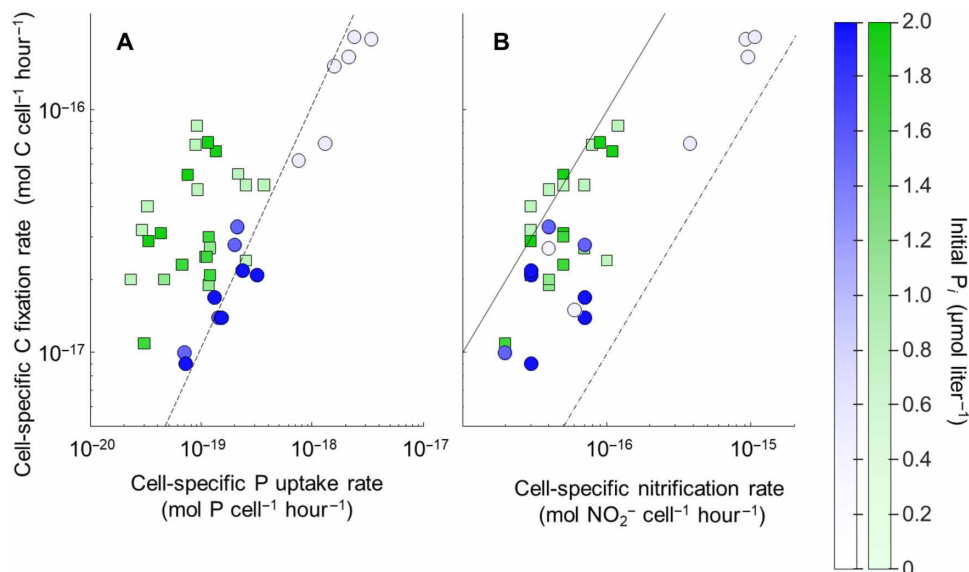
Fig. 1. Biogeochemical fluxes of *N. maritimus*. Cell-specific rates of C and P uptake (**A**) and nitrification (**B**) by *N. maritimus*. Data are shown for strains *SCM1* (green) and *NAOA6* (blue) during periods of linear increases in radiotracer incorporation ($N = 3$ for each data point). The color intensity represents the initial P_i concentration of the medium (0.1 to 2 μM) upon radiotracer addition. The dashed lines represent the Redfield ratio (106C:1P) in (A). The solid line in (B) represent a 1:1 relationship; the dotted line represents the 0.1:1 line previously assumed for scaling chemoautotrophic C fixation in the global oceans (see text).
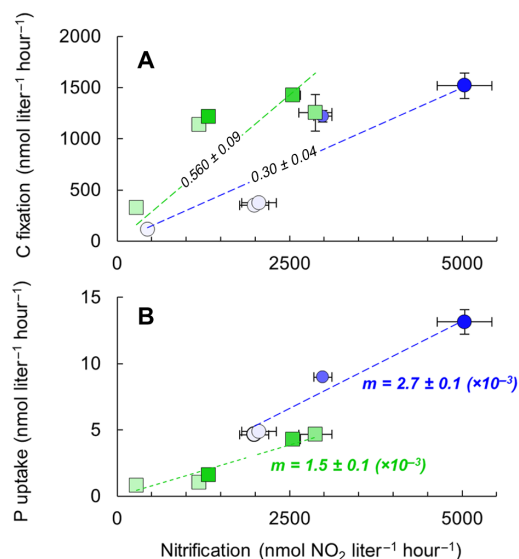
Fig. 2. C and P yields from nitrification by *N. maritimus*. Absolute rates of nitrification versus C fixation (**A**) and P_i uptake (**B**) by *N. maritimus*. The slopes of regression lines ($R^2 > 0.95$; $P < 0.01$) are given in italics (±SE) and represent the C and P yields from nitrification (C_0/N_n and P_0/N_n, respectively) for strains *SCM1* (green) and *NAOA6* (blue). The slope standard errors of the regressions shown in (B) are $< 1.5 \times 10^{-4}$. P_i amendment of the growth medium is indicated by the shade of the symbol as defined in Fig. 1. Error bars indicate propagated error of the 95% confidence interval of the slopes of linear rates of radiotracer incorporation or nitrite production over three to five time points among triplicate incubations ($N = 9$ to 15 for each data point; cf. fig. S3).

DISCUSSION

The aquarium and environmental strains of thaumarchaeon *N. maritimus* (*SCM1* and *NAOA6*, respectively) exhibited orders of magnitude differences in their physiological response to P_i limitation, which were simulated by culture conditions under which P_i

turnover time (τ_{PO4}) spanned three orders of magnitude (3 to 1500 hours). Thaumarchaea are not necessarily P limited in the deep ocean, where P_i ranges from 1 to 3 μM (*24*), and deep sea ecotypes may physiologically diverge still further than observed among our experimental strains. Nevertheless, our findings provide insight into how thaumarchaea complete for energy and nutrients derived from recycled production. The following discussion examines the implications of these findings for chemoautotrophic fluxes in the dark ocean as well as in the surface ocean, where nitrification is prominent, Thaumarchaea are most abundant (*1*, *11*), and P may be limiting (*13*).

### Cellular energy budget and C, N, P coupling

The alternative coupling of energetic, C fixation, and P assimilation fluxes exhibited by the two *N. maritimus* strains can be considered in terms of maintenance energy, which is the conceptual inverse of C yield from nitrification. Using the HP/HB pathway, thaumarchaea require only 4 mol ATP to fix 2 mol C with every turn of the cycle (*4*). On the basis of the measured C yields from nitrification and conversion factors of 268 kJ mol^{-1} NH_3 (*25*) and 40 kJ mol^{-1} ATP (*26*), we estimate that the aquarium strain *N. maritimus SCM1* required 6 to 15 mol ATP per mol C fixed. Under P starvation conditions, chemoautotrophic C fixation rates by the aquarium strain *N. maritimus SCM1* surmounted those of nitrification, yielding C_0/N_n values as high as 1.2 ± 0.2 (Table 1) and ATP requirements as low as 6 ± 1 per mol C. In contrast, *N. maritimus NAOA6* grown under P-replete conditions required relatively more energy (19 ± 4 mol ATP per mol C), and this demand increased up to 38 mol ATP per mol C fixed under P limitation ($C_0/N_n = 0.18 \pm 0.02$; Fig. 3D). Thus, whereas the aquarium strain *SCM1* appeared to prioritize C fixation without regard to P availability, the environmental strain devoted relatively more energy to maintenance and/or other cellular tasks.

The inferences based on apparent maintenance energy demand are consistent with the relative assimilation fluxes of C and P (C:P_{assim}),

Table 1. Coupled biogeochemical fluxes *of N. maritimus strains SCM1* and *NAOA6* and responses to P limitation. Minimum P_i turnover time (τ_{PO4}) and maximum specific affinity (α°_{PO4}) are indicated for periods of linear rates of radiotracer uptake in each incubation. Error estimates are propagated from the SE of the related slope of linear uptake, production, or nitrification rate and/or cell counts (cf. figs. S1 to S3 and table S1). PER, percent extracellular release of assimilated C or P. nd, no data.

Strain	Initial P_i (nM)	τ_{PO4} (hour)	α°_{PO4} (liter g^{-1}_{cell} $hour^{-1}$)	C_0/N_n (mol mol^{-1})	DOC_0/N_n (mmol mol^{-1})	PER-DOC (%)	P_0/N_n (mmol mol^{-1})	DOP_0/N_n (µmol mol^{-1})	PER-DOP (%)
SCM1	910	661 ± 24	4.4 ± 0.3	0.91 ± 0.06	43 ± 14	4.7 ± 2	1.2 ± 0.1	20 ± 3	1.6 ± 0.2
	740	100 ± 4	5.6 ± 1.6	0.56 ± 0.03	42 ± 3	7.6 ± 1	1.7 ± 0.1	13 ± 2	0.8 ± 0.1
	400	59 ± 3	13 ± 2.0	0.44 ± 0.07	45 ± 18	10.4 ± 4	1.6 ± 0.2	9 ± 1	0.6 ± 0.04
	190	125 ± 7	16 ± 3.3	0.95 ± 0.05	89 ± 32	9.4 ± 3	0.9 ± 0.03	12 ± 0.5	1.4 ± 0.1
	160	159 ± 3	66 ± 14	1.2 ± 0.2	nd	nd	2.9 ± 0.2	36 ± 19	1.2 ± 0.6
NAOA6	1870	101 ± 4	4.7 ± 1.6	0.30 ± 0.03	9 ± 2	3.1 ± 1	2.6 ± 0.3	11 ± 3	0.4 ± 0.1
	1220	95 ± 3	5.5 ± 3.4	0.41 ± 0.03	16 ± 4	4.0 ± 1	3.0 ± 0.1	26 ± 14	0.9 ± 0.5
	160	8.3 ± 3.7	998 ± 455	0.18 ± 0.02	nd	nd	2.4 ± 0.3	6 ± 2	0.2 ± 0.1
	130	16 ± 0.7	1124 ± 605	0.18 ± 0.02	nd	nd	2.3 ± 0.3	7 ± 2	0.3 ± 0.1
	<100*	3.2 ± 0.1	3167 ± 593	0.26 ± 0.03	nd	nd	nd	nd	nd

*For this incubation, >10% P_i was assimilated within 20 min of radiotracer addition and therefore too quickly to presume the initial P_i concentration for subsequent calculations.
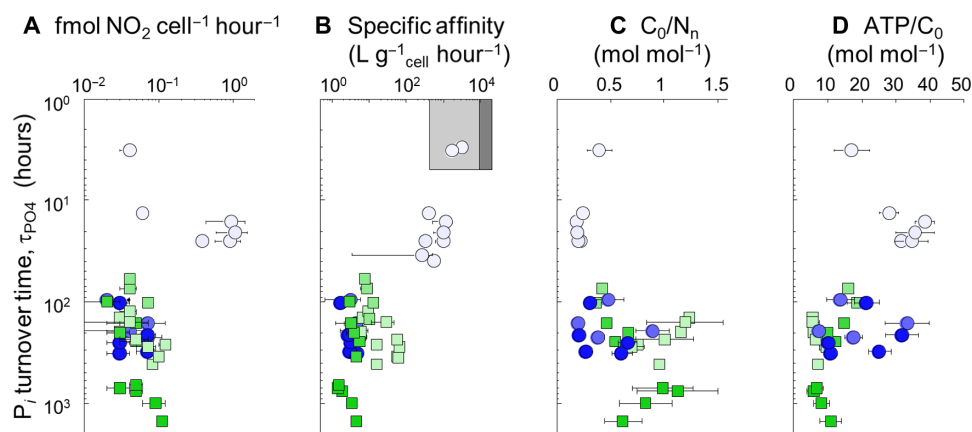
Fig. 3. Trends in *N. maritimus* physiology and P turnover time. Changes P_i turnover time (τ_{PO4}) in culture medium versus cell-specific nitrification rate (**A**), specific affinity for P_i (**B**), C yield (**C**), and ATP demand (**D**) of *N. maritimus*. Each data point represents the value determined for a single time point measurement during the growth phase and/or linear increases in radiotracer uptake (see Materials and Methods); error bars indicate propagated error of measurements of cell density, nitrite production, and/or fraction of ^{14}C or $^{33}P_i$ uptake (N = 3 for each data point). The shaded boxes in (B) indicate the range expected for pelagic bacterioplankton (gray) and cyanobacteria [dark gray; after (29)]. P_i amendment of the growth medium is indicated by the shade of the symbol as defined in Fig. 1.

which ranged up to an order of magnitude above Redfield stoichiometry for *N. maritimus SCM1* and dropped to 120C:1P only under conditions in which P-starved cells could no longer fix C (Fig. 1A and table S1). In contrast, C:P$_{assim}$ of the environmental strain *N. maritimus NAOA6* remained mostly constant and close to the Redfield ratio (106C:1P), even though the C:P of inorganic nutrient supply in experimental treatments ranged up to 20,000:1 (Fig. 1A). Therefore, the changes in biomass C:P stoichiometry of *N. maritimus NAOA6* induced by P stress were presumably manifested by altered nutrient allocation rather than nutrient acquisition strategy. By channeling P_i into intermediate metabolites, for example, *N. maritimus NAOA6* could presumably create a favorable gradient for faster uptake of P_i and thereby increase α°_{PO4} [cf. (27)]. These inferences are also con-

sistent with the conditioning of *N. maritimus SCM1* to a stable, aquarium environment ($\tau_{PO4} > 50$ hours; $\alpha^\circ_{PO4} < 70$ liter g^{-1}cell hour^{-1}), and the poise of strain *NAOA6* to adapt to fluctuating oceanographic conditions in the thermocline, where τ_{PO4} can span 5 to 100 hours over 30-m depth (28).

Together, these findings suggest that increased cellular power (Fig. 3A) may be a unique strategy of the environmental strain to fuel phenotypic alterations yielding higher α°_{PO4} as τ_{PO4} dropped below 50 hours (Fig. 3B). Furthermore, the C yield of nitrification by the environmental strain *N. maritimus NAOA6* rebounded to 0.26 ± 0.03 at $\tau_{PO4} < 5$ hours (Table 1 and Fig. 3C), suggesting a smaller maintenance energy requirement for P-starved cells that had adapted to P limitation. Combined with their high affinity for

Table 2. C, N, and P cell inventories of *N. maritimus NAOA6* grown in P-deplete or P-replete SCM medium. C:N:P values were all estimated by the same SEM-EDS instrumentation. Initial P_i concentrations of P-replete and P-deplete incubations were 1.4 to 1.7 and 0.35 to 0.37 μM.

SCM medium	C:N:P (molar)	fg C cell^{-1}	fg N cell^{-1}	fg P cell^{-1}
P-replete	58:10:1	34 ± 14	6.5 ± 2.8	1.5 ± 0.6
P-deplete	89:15:1	17 ± 6	3.4 ± 1.3	0.5 ± 0.2

ammonia (*3*), the adaptations demonstrated by the environmental strain should enable pelagic Thaumarchaeota to compete for limited nutrient and energy resources in ocean ecosystems dominated by recycled production. That is, (i) cell-specific nitrification rates were highest as τ_{PO4} decreased (Fig. 3A) to the range of time scales expected for the marine thermocline (*28*), and (ii) the P_i affinity of *N. maritimus NAOA6* is on the same order as bacterioplankton and also strategically lower than cyanobacteria (Fig. 3B) (*29*), who generate reduced N energy via primary production in oligotrophic surface waters. Achieving heightened P_i affinity appears to come at the cost of reduced C yield of nitrification (Fig. 3C); therefore, drastic changes in τ_{PO4} may contribute to the large variability in specific nitrification rates observed in the euphotic zone (*12*).

Martens-Habbena *et al.* (*3*) previously suggested that marine thaumarchaea rapidly achieve maximum ammonium oxidation rates with small maintenance energy demand because the half-saturation constant for ammonium is constitutively low. It follows that the C yield of nitrification should not decrease for energy limited cells, which is similar to the response of *N. maritimus NAOA6* adapted to $\tau_{PO4} < 5$ hours (Table 1 and Fig. 3C); in fact, C yield increased at lower cell-specific nitrification rates (fig. S4). Because marine thaumarchaea in the bathypelagic ocean are likely limited by energy and therefore intrinsically adapted for rapid ammonium uptake (*3*), we expect that the maintenance energy requirement and C yield of nitrification of pelagic and bathypelagic populations should be independent of transient or limiting concentrations of ammonium, but this remains to be tested.

Implications of thaumarchaeal C fixation efficiency

Previous studies have estimated thaumarchaeal C fixation in the dark ocean [text S1; (*2*, *6*, *7*)] by invoking the C yield from nitrification (C_0/N_n) for an ammonia-oxidizing bacterium (AOB) [*N. marina*; $C_0/N_n = 0.1$; (*8*, *9*)], but nitrifying thaumarchaea, i.e., *N. maritimus*, can be up to 10 times more efficient at fixing C (Table 1). High variability in C_0/N_n was evident between the aquarium and environmental strains of *N. maritimus* and in their response to P limitation (Fig. 3C and fig. S5); moreover, the C yield of uncultured, bathypelagic ecotypes may differ from those dwelling nearer the euphotic zone. Nevertheless, to estimate the significance of thaumarchaeal nitrification in the global C budget (Table 3), we apply a C_0/N_n value determined via linear regression of all incubations of the environmental archaeon *N. maritimus NAOA6* ($0.30 ± 0.04$, $R^2 = 0.94$, $P < 0.01$; Fig. 2A). This C_0/N_n value is threefold higher than previously assumed and is consistent with marine archaea fixing C via the more efficient HP/HB pathway versus the Calvin-Benson cycle used by AOB [cf. (*8*, *9*)

According to Redfield stoichiometry, mineralization of sinking particles in the ocean should yield 16 mol of reduced N (i.e., ammonia) for 106 mol of C respired. Ammonium may be recycled to support primary production, either directly or following nitrification [i.e., regenerated production; (*12*, *14*)], with the latter comprising the additional C fixation fluxes of nitrifiers that counter respired CO_2. Applying the measured C_0/N_n for archaeal nitrification (0.30) to a Redfieldian mineralization flux (106C:16N), we approximate that marine thaumarchaea recycle 4.5% of organic C mineralized in the oceans (Eq. 1)

$$\text{Thaumarchaeal recycling } (\%DIC_{remin}) = C_0/N_n \times 16/106 \quad (1)$$

This percentage is likely lower in the euphotic zone, where thaumarchaea compete with phototrophs for ammonium; however, given the preferential degradation of N relative to C from sinking particles (*30*), this is likely a conservative estimate of C recycling efficiency by a steadfast population of nitrifiers across the global bathypelagic ocean.

By assuming a mineralization rate of reduced N exported to the ocean interior, a flux estimated at 92 Tmol N year^{-1} [(*2*) after (*31*)] to 330 Tmol N year^{-1} [cf. (*7*)], and the revised C yield for archaeal nitrification, we arrive at a dark ocean C fixation flux ranging from 0.33 to 1.2 Pg C year^{-1} (Table 3). This estimate approaches the upper range of direct measurements of dark ocean chemoautotrophy [0.8 to 1.2 Pg C year^{-1}; (*5*, *6*, *32*); see text S1], without having to invoke additional sources of energy to fuel C fixation. However, nitrite-oxidizing bacteria (NOB) are also known to be active below the euphotic zone and would further oxidize the same N atoms to contribute an additive C fixation flux [~1 Pg C year^{-1}; (*32*, *33*)]. NOB are larger than *N. maritimus*, demand roughly an equivalent amount of ATP for each turn of their C fixation cycle (Fig. 3D) (*4*, *33*), and in situ, single cell C and N uptake studies suggest NOBs may have a greater C yield than thaumarchaea (*32*, *34*). Therefore, if the integrated ammonium and nitrite oxidation fluxes in the dark ocean transpire with a C yield of ~ 0.3, then the amount of remineralized C that is recycled into nitrifier biomass ($\%DIC_{remin}$) could theoretically approach 9% (Eq. 1). This amounts to ~0.86 Pg C year^{-1} if we conservatively assume an oceanic C export flux of 9.55 Pg C year^{-1} (*31*). C fixation by meso- and bathypelagic nitrifiers may therefore account for at least 70% of the upper estimate of total dark ocean chemoautotrophy.

Chemoautotrophs were conservatively estimated to respire 43% of ammonia in waters above the thermocline, and thaumarchaea are also known to derive energy from other sources of reduced N, such as urea and cyanate (*35*). This translates to a C fixation rate upward of 0.8 Pg C year^{-1} (Table 3) and on the same order as dark ocean fluxes. Therefore, we estimate that global ocean C fixation supported by archaeal nitrification ranges from 1 to 2 Pg C year^{-1}, or roughly 2 to 4% of net primary production [54 Pg C year^{-1}; (*31*)]. If this flux is integrated over a standing stock of 10^{28} thaumarchaeal cells in the ocean (*1*) with a C content of 12.9 fg cell^{-1} (*22*), we estimate an average thaumarchaeal turnover time, or the residence time of C as thaumarchaeal biomass, on the order of 3 to 10 weeks, with growth rates ranging from 0.002 day^{-1} in the deep ocean to 0.4 day^{-1} in near-shore ecosystems (Table 3).

Thaumarchaeal cycling of P and DOM

Our dual radiotracer approach provided parallel rate measurements of P assimilation and DOM release by *N. maritimus* to further consider the coupling of these fluxes to nitrification in the global oceans (Table 3). P_i assimilation by Thaumarchaeota (ca. 20 Tg P year^{-1}; Table 3) is on the same order as annual riverine input of P_i (*24*) and roughly 4% of that consumed by photoautotrophs in the surface

Table 3. Chemoautotrophic growth rate, uptake, and chemosynthate release fluxes of C (Tg year⁻¹) and P (Gg year⁻¹) in the global ocean. Estimates are based on measured ratios of *N. maritimus NAOA6* fluxes of C and P relative to nitrite production during radiotracer experiments (Table 1 and fig. S5) and respiration rates of organic C in the euphotic or dark oceans [after (*2*, *31*); see text S1]. In the euphotic zone, the fluxes correspond to the proportion of reduced N from respiration that is assumed to be available for nitrification [43%, after (*2*, *12*)]. The range of total C or P fluxes in the dark ocean corresponds to the low and high estimates of total N mineralization flux (92 or 330 Tmol N year⁻¹; see text). Relatively lower C and P uptake fluxes observed in response to P limitation are accounted for by assuming 13% of the open ocean euphotic zone is P limited [i.e., the N. Atlantic Equatorial and Subtropical Gyre; 15°S to 45°N; (*13*)]. Thaumarchaeal growth rates (day⁻¹) are estimated on the basis of population densities reported by (*11*), ocean surface areas (*31*) and depths of hypsometric regions (*43*), C content of 12.9 fg cell⁻¹ (*22*), and the C fixation fluxes reported here for each region.

Zone	Flux	Near-shore	Shelf	Slope	Open	Total
Euphotic	Growth rate (day⁻¹)	0.413	0.209	0.081	0.049	–
	C fixation (Tg year⁻¹)	48	39	60	676	824
	P uptake (Gg year⁻¹)	1.2	1.0	1.4	16.9	20
	DOC release (Tg year⁻¹)	2.1	1.7	2.6	30.4	37
	DOP release (Gg year⁻¹)	0.008	0.006	0.010	0.106	0.13
Dark	Growth rate (day⁻¹)	nd	0.099	0.006	0.002	–
	C fixation (Tg year⁻¹)	1.8	15	29	284	330–1190
	P uptake (Gg year⁻¹)	0.04	0.37	0.70	6.7	8–29
	DOC release (Tg year⁻¹)	0.08	0.66	1.24	12.1	14–51
	DOP release (Gg year⁻¹)	0.0003	0.003	0.005	0.046	0.05–0.19

ocean, assuming Redfield stoichiometry and net primary production flux of 54 Pg C year⁻¹ (*31*). P_i uptake of by Thaumarchaeota in the deep ocean is roughly equal in magnitude and could counterbalance 4.3% of P mineralized from sinking particles, assuming molar N:P ratios of 16:1 for mineralization (Redfield) and P_0/N_n of 1:370 (Fig. 2B; cf. Eq. 1). This flux contributes to the P packaging onto particles known to be mediated by heterotrophic bacteria, having important consequences for the reactivity of organic P in the bathypelagic ocean and eventual burial in marine sediments (*36*).

The proportional release of DOC by *N. maritimus NAOA6* (5 ± 2%; tables S2 and S3) was similar to that reported for microbial photoautotrophs [i.e., cyanobacteria; (*37*)] and suggests that thaumarchaea release 20 to 90 Tg C as DOC into the deep ocean each year (Table 3). A similar estimate of 14 to 51 Tg C year⁻¹ can be extrapolated by applying the ratio of DOC:NO₂ produced by *N. maritimus NAOA6* (0.013:1; Table 1 and fig. S5) to the complete oxidation of the sinking flux of reduced N to the ocean interior (Table 3). As such, DOC release by thaumarchaea likely amounts to only a small fraction of the total estimated organic C supplied to the deep ocean via sinking particles and advected DOC [10 to 26 Pg C year⁻¹; (*31*, *38*)], but may nevertheless represent a large portion of the labile DOC pool in the bathypelagic ocean [cf. (*9*)]. Similarly, the DOP:NO₂ ratio (Table 1 and fig. S5) predicts a total release of roughly 0.32 Tg P y¹ into the global ocean (Table 3). Given the capacity for thaumarchaea to metabolize phosphonates (*16*), this flux may contribute up to 10% of reduced compounds in the oceanic P redox cycle (*39*).

While DOM produced by thaumarchaea is presumably labile (*20*), DOM release represents only a fraction of C and P assimilated into thaumarchaeal biomass, which may turn over on time scales longer than 1 year in the bathypelagic ocean (ca. 450 days; Table 3). The rates and yields reported for *N. maritimus* cultures in the current study represent an incremental step toward modeling bathypelagic chemoautotrophs, who operate at lower temperature, higher pressure, and may use other reduced substrates [e.g., (*10*, *33*)]. At present, our empirical evidence recommends that biogeochemical budgets include chemoautotrophic recycling fluxes driven by reduced N that mitigate at least 4.5% of detrital organic C respiration and transform 4.3% of detrital P into new P substrates.

MATERIALS AND METHODS
Experimental design and cultivation
Stock cultures (30 ml) of *N. maritimus* strains *SCM1* and *NAOA6* were grown aerobically at 28°C in 30 ml of SCM (*15*) containing 1 mM ammonium and 2 µM phosphate and were continuously transferred to sterile SCM medium when nitrite concentrations approached 1 mM. For the ³³P and ¹⁴C uptake experiments (scheme S1), large batch cultures were initiated by inoculating cells from stock cultures in the growth phase (25 to 30 ml; ca. 10^{7-8} cells) into SCM media (0.8 liters) containing 0.1 to 1.6 µM P_i. Sterile SCM medium that was not amended with KH_2PO_4 still exhibited measureable quantities of P_i (ca. 130 nM), likely deriving from impurities in other components of the artificial seawater medium. After inoculation, nitrite concentrations in culture media were measured every 1 to 3 days via colorimetry to monitor growth after (*15*). Aliquots (45 ml) of the experimental batch culture were transferred into 13 sterile 50-ml plastic screw-top centrifuge tubes (Sarstedt, Germany) after the end lag phase growth, typically after 7 to 10 days, as suggested by nitrite concentrations increasing above a threshold of 0.1 mM. In addition to the radiotracer experiments, stock cultures of *N. maritimus NAOA6* were also inoculated into triplicate batch cultures for cellular P quantification and SEM-EDS analyses (scheme S1).

Cellular P quotas and SEM-EDS analysis
N. maritimus NAOA6 was grown in triplicate, nonspiked batch cultures (0.8 liter SCM medium) amended to simulate P-deplete (0.35 to 0.37 µM P_i) or P-replete (1.4 to 1.7 µM P_i) conditions, and samples were collected for determination of P_i, total P (TP), and total dissolved P (TDP) at the initial and final time points of cultivation. Growth was monitored via nitrite evolution and epifluorescence microscopy of cells fixed in 1.6% formalin, filtered onto a 0.2-µm cellulose membrane (Whatman), and stained with SYBR Green I. At least 10 magnification fields (100×) were counted. *N. maritimus NAOA6* cells were harvested via centrifugation (4800g for 1 hour) when nitrite concentrations in all replicate P-deplete or P-replete cultures increased above a threshold of 0.3 or 0.5 mM, respectively, as suggestive of cells having entered the growth phase. Most of the

supernatant was decanted and the pelleted cells were resuspended in a small volume (<10 ml) of culture medium remaining in the bottle (i.e., cell concentrate). Aliquots of the cell concentrate samples were analyzed for P_i, TP, and TDP as described below. The remaining volume of the cell concentrate was fixed with formaldehyde (final concentration 1.6%) and stored at 4°C. Cell density of the concentrated, fixed sample was determined via staining SYBR Green I as above.

For SEM-EDS analysis, aliquots of concentrated and fixed *N. maritimus NAOA6* cells (1 to 1.5 ml) were pelleted for 20 min at 20,000g in 2-ml centrifuge tubes and then washed three times by resuspending in 1 ml of deionized water and repeating the centrifugation step. The washed and pelleted cells were then resuspended in 5 µl of water and air dried onto a silicon wafer. For P-limited cells that were also subjected to cell weight analysis, cells were washed twice by pelleting at 3000g for 5 min, resuspended in 1 ml of Milli-Q water, and a 30-µl aliquot was air dried for 2 hours onto a silicon wafer. After dehydration, the silicon wafers were mounted onto electrically conductive adhesive tags (Leit-Tab, Plano GmbH, Wetzlar, Germany) for elemental ratio analysis.

C:N, C:P, and N:P elemental ratios were obtained using a scanning electron microscope (Quanta FEG 250, FEI) equipped with an energy-dispersive x-ray spectroscopy (EDS) double detector system (QUANTAX EDS, Bruker Nano GmbH). The detectors (XFlash 6/30) had a detector area of 30 mm^2 and an energy resolution at Mn K α line of <123 eV, allowing the quantification of most light elements. To check the performance of the EDS system, the NBS SRM 1155 ANSI 316 stainless steel standard was used. The EDS spectra were tested using an accelerating voltage of 10 and 20 kV to see if other elements with a higher atomic number than Ca were present in the sample. A 10-kV acceleration voltage was used for further measurements, which had a reduced penetration depth. The elemental ratios were calculated for five object fields using the QUANTAX 400 software (version 1.9, Bruker), in which the elements C, N, O, Na, Mg, Al, P, S, Cl, K, and Ca were included.

Phosphate and bicarbonate concentration

Samples (10 ml) for P_i, TP, and TDP were collected from culture media using a sterile pipette. TDP samples were gently filtered through a Luer lock filter (Sartorius; pore size, 0.1 µm). P_i, TDP, and TP samples were immediately frozen at −20°C. Concentrations of P_i, TP, and TDP were determined via the molybdenum-blue colorimetric method (40) on a QuAAtro AA3 Dual Channel Total P & Orthophosphate Autoanalyzer with a 100-cm Liquid Waveguide Capillary Cell (Seal Analytic, Germany). DOP concentrations were estimated as TDP minus P_i and were corrected for the concentration of DOP measured in sterile SCM medium (0.07 µM). Precision of the P_i, TP, and TDP measurements was 0.75% (1 σ coefficient of variation), and the minimum quantifiable limit for P_i was 20 nM, and 41 nM for TP and TDP. Cell P quota estimates are derived from the TP of cell concentrate minus the TDP value of the culture media at the final time point of cultivation.

For total dissolved inorganic carbon, samples of culture medium (1.8 ml) were filled into an annealed (550°C) vial and sealed without air bubbles and stored at 4°C. The dissolved inorganic carbon (DIC) contents were determined with a multi N/C 2100S analyzer from Analytik Jena. Immediately before the measurement, 150 µl of each sample was discarded and automatically replaced by 50 µl of 10% H_3PO_4. The outgassing CO_2 was analyzed via nondispersive infra-

red detection in triplicate, and DIC concentrations were calculated based on a series of calibration standards prepared from a stock solution 1000 mg liter^{-1} from ULTRA Scientific (IQC106).

^{33}P and ^{14}C uptake experiments and activity measurement

For each ^{33}P or ^{14}C uptake experiment, five 45-ml treatment cultures, including three live treatments, one killed control, and one blank, were spiked with either ^{33}P-labeled carrier-free, phosphoric acid or ^{14}C-labeled bicarbonate (Hartmann Analytic GmbH, Braunschweig, Germany) to an activity of ca. 150 kBq. In parallel to the 10 radiotracer uptake experiments (five each for ^{33}P and ^{14}C uptake), three non-spiked treatments (45 ml) were grown aerobically at 28°C to monitor growth via nitrite evolution as well as epifluorescence microscopy (scheme S1). Briefly, cells were enumerated in at least 10 magnification fields (100×) after fixing with formaldehyde (final concentration, >1.6% v/v), filtering onto 0.2-µm polycarbonate membranes (Isopore GTTP; 25 mm), and staining with 4′,6-diamidino-2-phenylindole. The experimental blanks served as controls for abiotic ^{33}P or ^{14}C incorporation into particles and were prepared by filtering 45 ml of the culture medium through a Luer lock syringe filter (Sartorius; pore size, 0.1 µm) before spiking with radiotracer. The killed control treatments were prepared by incubating culture aliquots at 80°C for >45 min and then cooling to room temperature before the radiotracer spike.

After spiking, the centrifuge tubes were gently shaken for 10 s, and samples were collected for both time point zero (t_0; 5 ml) and total radioactivity ($^{33}A_{total}$ and $^{14}A_{total}$; Bq ml^{-1}). For the latter, samples (100 µl) were added directly to 6-ml scintillation vials and amended with 5 ml of scintillation fluid. For all spiked treatments, culture aliquots (3 to 5 ml) were collected at time points distributed over ca. 200 hours following label addition, fixed with formaldehyde in the filtration tower to a final concentration of 2 to 4% for 20 min, and then vacuum filtered over 0.2-µm polycarbonate membranes (Isopore GTTP; 25 mm). The filters were then rinsed three times with 5 ml of MilliQ water to remove residual P_i. Each filter was then transferred to a 6-ml scintillation vial and amended with 5 ml of scintillation fluid (Irgasafe Plus, PerkinElmer). The volume-normalized radioactivity on the filter ($^{33}A_{cell}$ or $^{14}A_{cell}$; Bq ml^{-1}) was measured on a Packard 2500 TR scintillation counter, with quench correction (tSIE/AEC based on ^{14}C quench standards). During each time point sampling, while the spiked culture aliquots were being fixed with formaldehyde, nitrite and cell density samples were collected from the parallel nonspiked, live treatments. Nitrite was measured as described above for stock cultures. Cell count samples (1 ml) were fixed by adding 0.1 ml of 20% formaldehyde and stored at 4°C until analysis (as above).

Determination of C and P assimilation rates, P_i turnover time, and specific affinity for P_i

The fraction (f) of bicarbonate or P_i assimilated into biomass was calculated as the ratio of activity in biomass (i.e., on the filter; $^{14}A_{cell}$ or $^{33}A_{cell}$, respectively) to total radioactivity added (i.e., $f = {}^{14}A_{cell}/{}^{14}A_{total}$ or $^{33}A_{cell}/{}^{33}A_{total}$). The mean fractional uptake for triplicate measurements was corrected by that of the killed control. Absolute quantities of assimilated bicarbonate and P_i were determined on the basis of the fractional uptake estimates (f, unitless) and the initial concentration (mol liter^{-1}) of these nutrients in the culture medium before partitioning into individual incubations and at most 2 hours before radiotracer addition. Rates of C and P assimilation were determined

via linear regression using MATLAB 2014a for the time interval over which the culture was in the growth phase, or, for experiments exhibiting little or no increase in cell density, rates were determined over the interval of linear increases in the radiotracer uptake (i.e., first-order uptake). Errors in rate estimates are based on the 95% confidence interval of the slope coefficients (see Statistical analysis). Rates of cell-specific C and P uptake and nitrite production were determined for specific time points based on estimates of cell density (cell liter^{-1}) and the increase in assimilated bicarbonate or P$_i$ since the previous time point. P$_i$ turnover time (τ_{PO4}; in hours) was calculated for each time point (t) according to (41)

$$\tau_{PO4}(h) = t \times [-\ln(1-f)]^{-1} \qquad (2)$$

The specific affinity ($\alpha°$; liter g$_{cell}^{-1}$ hour^{-}1 or liter nmol P^{-1} hour^{-1}) of *N. maritimus* for P$_i$ was calculated according to (27)

$$\alpha°(L\,g^{-1}_{cell}\,h^{-1}) = [\tau_{PO4} \times \text{cell density}]^{-1} \qquad (3)$$

N. maritimus cell abundance was converted to either P content (nmol P), based on cellular P quota determined in P-deplete or P-replete medium, or cell weight [g$_{cell}$; 24.6 fg cell^{-1}; (22)]. Propagated error of $\alpha°$ was based on uncertainty in measurements of cell abundance, the fractional uptake of radiotracer, and cellular P quota.

Determination of DOP and DOC production rates

Estimates of DOP and DOC release into culture media were measured at the end of the experiments and, thus, integrate accumulation during incubation period. At the final time point of the radiotracer assay, the remaining volumes of the live, killed control, and blank treatments (3 to 6 ml) were fixed in 1 to 2% formaldehyde for >20 min, filtered through a Luer lock syringe filter (Sartorius; pore size, 0.1 μm), and collected into 15-ml centrifuge tubes or 20-ml scintillation vials for DO^{33}P or DO^{14}C analysis, respectively. For measurements of DOP radioactivity ($^{33}A_{DOP}$), P$_i$ was first coprecipitated with magnesium from the medium by adding 0.15 ml of 3 M NaOH (pH 11) and centrifuging at 700g for 45 min to remove the spiked ^{33}P$_i$ after (42). The supernatant was decanted into 20-ml scintillation vials and amended with twice the volume of scintillation fluid. For DOC radioactivity measurements ($^{14}A_{DOC}$), the filtrate was acidified to pH 2 by adding 30 μl of concentrated hydrochloric acid and bubbled with N$_2$ for >5 min to remove inorganic ^{14}C. The mean $^{33}A_{DOP}$ or $^{14}A_{DOC}$ activity of triplicate live treatments was corrected by of the corresponding killed control. For incubations of *NAOA6* at 130 and 160 nM P$_i$, the sparging time was obviously too short (i.e., <25 min), and these anomalously high values are not reported. For *NAOA6* and SCM1 incubations at <100 μM P$_i$, $^{14}A_{cell}$ values were too low to provide reliable estimates of DOC release. The concentration of DOP or DOC produced during the experiment was determined as the product of the fraction of total radiotracer ($^{33}A_{total}$ or $^{14}A_{total}$; Bq ml^{-1}) that had accumulated as extracellular organic matter ($^{33}A_{DOP}$ or $^{14}A_{DOC}$; Bq ml^{-1}) and the initial P$_i$ (P$_{i0}$) or DIC concentration (Eq. 4). These concentration values were normalized by the entire time of incubation (t) and maximum cell density (cell$_{max}$) observed during growth and are thus considered as conservative estimates of cell-specific DOM production rate, as we cannot constrain the timing of DOM release. DOP and DOC release are also expressed as percent extracellular release (PER; Eq. 5), which was calculated by normalizing the $^{33}A_{DOP}$ and $^{14}A_{DOC}$ at the final time point to the maximum

activity of biomass observed during the course of the experiment ($^{33}A_{cell}$ or $^{14}A_{cell}$)

$$\text{DOP release rate (mol P cell}^{-1}\text{d}^{-1}) = P_{i0} \times {}^{33}A_{DOP}/{}^{33}A_{total} \times \text{cell}_{max}^{-1} \times t^{-1} \qquad (4)$$

$$\text{PER}_{DOP}(\%) = 100 \times {}^{33}A_{DOP}/{}^{33}A_{cell} \qquad (5)$$

Statistical analysis

Reported 95% confidence intervals, R^2 statistics, and P values of linear regressions were computed using the MATLAB R2014a regress function. Significance differences (P value) reported for radiotracer uptake or release as DOP or DOC between live, killed, and blank treatments refer to the probability associated with a homoscedastic Student's t test.

REFERENCES AND NOTES

1. M. B. Karner, E. F. DeLong, D. M. Karl, Archaeal dominance in the mesopelagic zone of the Pacific Ocean. *Nature* **409**, 507–510 (2001).
2. J. J. Middelburg, Chemoautotrophy in the ocean. *Geophys. Res. Lett.* **38**, L24604 (2011).
3. W. Martens-Habbena, P. M. Berube, H. Urakawa, J. R. de la Torre, D. A. Stahl, Ammonia oxidation kinetics determine niche separation of nitrifying Archaea and Bacteria. *Nature* **461**, 976–979 (2009).
4. M. Könneke, D. M. Schubert, P. C. Brown, M. Hügler, S. Standfest, T. Schwander, L. Schada von Borzyskowski, T. J. Erb, D. A. Stahl, I. A. Berg, Ammonia-oxidizing archaea use the most energy-efficient aerobic pathway for CO$_2$ fixation. *Proc. Natl. Acad. Sci. U.S.A.* **111**, 8239–8244 (2014).
5. G. J. Herndl, T. Reinthaler, E. Teira, H. van Aken, C. Veth, A. Pernthaler, J. Pernthaler, Contribution of *Archaea* to total prokaryotic production in the deep Atlantic Ocean. *Appl. Environ. Microbiol.* **71**, 2303–2309 (2005).
6. T. Reinthaler, H. M. van Aken, G. J. Herndl, Major contribution of autotrophy to microbial carbon cycling in the deep North Atlantic's interior. *Deep. Res. Part II* **57**, 1572–1580 (2010).
7. C. Wuchter, B. Abbas, M. J. L. Coolen, L. Herfort, J. van Bleijswijk, P. Timmers, M. Strous, E. Teira, G. J. Herndl, J. J. Middelburg, S. Schouten, J. S. Sinninghe Damsté, Archaeal nitrification in the ocean. *Proc. Natl. Acad. Sci. U.S.A.* **103**, 12317–12322 (2006).
8. H. E. Glover, The relationship between inorganic nitrogen oxidation and organic carbon production in batch and chemostat cultures of marine nitrifying bacteria. *Arch. Microbiol.* **142**, 45–50 (1985).
9. L. Tijhuis, M. C. M. Van Loosdrecht, J. J. Heijnen, A thermodynamically based correlation for maintenance gibbs energy requirements in aerobic and anaerobic chemotrophic growth. *Biotechnol. Bioeng.* **42**, 509–519 (1993).
10. E. Guerrero-Feijóo, E. Sintes, G. J. Herndl, M. M. Varela, High dark inorganic carbon fixation rates by specific microbial groups in the Atlantic off the Galician coast (NW Iberian margin). *Environ. Microbiol.* **20**, 602–611 (2018).
11. D. L. Kirchman, H. Elifantz, A. I. Dittel, R. R. Malmstrom, M. T. Cottrell, Standing stocks and activity of Archaea and Bacteria in the western Arctic Ocean. *Limnol. Oceanogr.* **52**, 495–507 (2007).
12. A. Yool, A. P. Martin, C. Fernández, D. R. Clark, The significance of nitrification for oceanic new production. *Nature* **447**, 999–1002 (2007).
13. C. M. Moore, M. M. Mills, K. R. Arrigo, I. Berman-Frank, L. Bopp, P. W. Boyd, E. D. Galbraith, R. J. Geider, C. Guieu, S. L. Jaccard, T. D. Jickells, J. La Roche, T. M. Lenton, N. M. Mahowald, E. Marañón, I. Marinov, J. K. Moore, T. Nakatsuka, A. Oschlies, M. A. Saito, T. F. Thingstad, A. Tsuda, O. Ulloa, Processes and patterns of oceanic nutrient limitation. *Nat. Geosci.* **6**, 701–710 (2013).
14. R. W. Eppley, B. J. Peterson, Particulate organic matter flux and planktonic new production in the deep ocean. *Nature* **282**, 677–680 (1979).
15. M. Könneke, A. E. Bernhard, J. R. de la Torre, C. B. Walker, J. B. Waterbury, D. A. Stahl, Isolation of an autotrophic ammonia-oxidizing marine archaeon. *Nature* **437**, 543–546 (2005).
16. C. B. Walker, J. R. de la Torre, M. G. Klotz, H. Urakawa, N. Pinel, D. J. Arp, C. Brochier-Armanet, P. S. G. Chain, P. P. Chan, A. Gollabgir, J. Hemp, M. Hügler, E. A. Karr, M. Könneke, M. Shin, T. J. Lawton, T. Lowe, W. Martens-Habbena, L. A. Sayavedra-Soto, D. Lang, S. M. Sievert,

A. C. Rosenzweig, G. Manning, D. A. Stahl, *Nitrosopumilus maritimus* genome reveals unique mechanisms for nitrification and autotrophy in globally distributed marine crenarchaea. *Proc. Natl. Acad. Sci. U.S.A.* **107**, 8818–8823 (2010).

17. D. A. Stahl, J. R. de la Torre, Physiology and diversity of ammonia-oxidizing archaea. *Annu. Rev. Microbiol.* **66**, 83–101 (2012).

18. A. E. Ingalls, S. R. Shah, R. L. Hansman, L. I. Aluwihare, G. M. Santos, E. R. M. Druffel, A. Pearson, Quantifying archaeal community autotrophy in the mesopelagic ocean using natural radiocarbon. *Proc. Natl. Acad. Sci. U.S.A.* **103**, 6442–6447 (2006).

19. R. L. Hansman, S. Griffin, J. T. Watson, E. R. M. Druffel, A. E. Ingalls, A. Pearson, L. I. Aluwihare, The radiocarbon signature of microorganisms in the mesopelagic ocean. *Proc. Natl. Acad. Sci. U.S.A.* **106**, 6513–6518 (2009).

20. B. Bayer, R. L. Hansman, M. J. Bittner, B. E. Noriega-Ortega, J. Niggemann, T. Dittmar, G. J. Herndl, Ammonia-oxidizing archaea release a suite of organic compounds potentially fueling prokaryotic heterotrophy in the ocean. *bioRxiv* , 558726 (2019).

21. F. J. Elling, M. Könneke, M. Mußmann, A. Greve, K.-U. Hinrichs, Influence of temperature, pH, and salinity on membrane lipid composition and TEX_{86} of marine planktonic thaumarchaeal isolates. *Geochim. Cosmochim. Acta* **171**, 238–255 (2015).

22. A. Khachikyan, J. Milucka, S. Littmann, S. Ahmerkamp, T. Meador, M. Könneke, T. Burg, M. M. M. Kuypers, Direct cell mass measurements expand the role of small microorganisms in nature. *Appl. Environ. Microbiol.* **85**, e00493-19 (2019).

23. C. M. Godwin, J. B. Cotner, Aquatic heterotrophic bacteria have highly flexible phosphorus content and biomass stoichiometry. *ISME J.* **9**, 2324–2327 (2015).

24. C. R. Benitez-Nelson, The biogeochemical cycling of phosphorus in marine systems. *Earth Sci. Rev.* **51**, 109–135 (2000).

25. J. P. Amend, E. L. Shock, Energetics of overall metabolic reactions of thermophilic and hyperthermophilic Archaea and Bacteria. *FEMS Microbiol. Rev.* **25**, 175–243 (2001).

26. R. K. Thauer, K. Jungermann, K. Decker, Energy conservation in chemotrophic anaerobic bacteria. *Bacteriol. Rev.* **41**, 100–180 (1977).

27. D. K. Button, Nutrient uptake by microorganisms according to kinetic parameters from theory as related to cytoarchitecture. *Microbiol. Mol. Biol. Rev.* **62**, 636–645 (1998).

28. T. Tanaka, F. Rassoulzadegan, T. F. Thingstad, Orthophosphate uptake by heterotrophic bacteria, cyanobacteria, and autotrophic nanoflagellates in Villefranche Bay, northwestern Mediterranean: Vertical, seasonal, and short-term variations of the competitive relationship for phosphorus. *Limnol. Oceanogr.* **49**, 1063–1072 (2004).

29. T. Tanaka, F. Rassoulzadegan, T. F. Thingstad, Measurements of phosphate affinity constants and phosphorus release rates from the microbial food web in Villefranche Bay, northwestern Mediterranean. *Limnol. Oceanogr.* **48**, 1150–1160 (2003).

30. G. A. Knauer, J. H. Martin, K. W. Bruland, Fluxes of particulate carbon, nitrogen, and phosphorus in the upper water column of the northeast Pacific. *Deep Sea Res. Part A Oceanogr. Res. Pap.* **26**, 97–108 (1979).

31. J. P. Dunne, J. L. Sarmiento, A. Gnanadesikan, A synthesis of global particle export from the surface ocean and cycling through the ocean interior and on the seafloor. *Global Biogeochem. Cycles* **21**, GB4006 (2007).

32. M. M. Varela, H. M. van Aken, E. Sintes, T. Reinthaler, G. J. Herndl, Contribution of *Crenarchaeota* and *Bacteria* to autotrophy in the North Atlantic interior. *Environ. Microbiol.* **13**, 1524–1533 (2011).

33. M. G. Pachiadaki, E. Sintes, K. Bergauer, J. M. Brown, N. R. Record, B. K. Swan, M. E. Mathyer, S. J. Hallam, P. Lopez-Garcia, Y. Takaki, T. Nunoura, T. Woyke, G. J. Herndl, R. Stepanauskas, Major role of nitrite-oxidizing bacteria in dark ocean carbon fixation. *Science* **358**, 1046–1051 (2017).

34. K. Kitzinger, H. K. Marchant, L. A. Bristow, C. W. Herbold, C. C. Padilla, A. T. Kidane, S. Littmann, H. Daims, P. Pjevac, F. J. Stewart, M. Wagner, M. M. M. Kuypers, Single cell analyses reveal contrasting life strategies of the two main nitrifiers in the ocean. *Nat. Commun.* **11**, 767 (2020).

35. K. Kitzinger, C. C. Padilla, H. K. Marchant, P. F. Hach, C. W. Herbold, A. T. Kidane, M. Könneke, S. Littmann, M. Mooshammer, J. Niggemann, S. Petrov, A. Richter, F. J. Stewart, M. Wagner, M. M. M. Kuypers, L. A. Bristow, Cyanate and urea are substrates for nitrification by Thaumarchaeota in the marine environment. *Nat. Microbiol.* **4**, 234–243 (2019).

36. S. Sokoll, T. G. Ferdelman, M. Holtappels, T. Goldhammer, S. Littmann, M. H. Iversen, M. M. M. Kuypers, Intense biological phosphate uptake onto particles in subeuphotic continental margin waters. *Geophys. Res. Lett.* **44**, 2825–2834 (2017).

37. J. W. Becker, P. M. Berube, C. L. Follett, J. B. Waterbury, S. W. Chisholm, E. F. DeLong, D. J. Repeta, Closely related phytoplankton species produce similar suites of dissolved organic matter. *Front. Microbiol.* **5**, 111 (2014).

38. P. A. del Giorgio, C. M. Duarte, Respiration in the open ocean. *Nature* **420**, 379–384 (2002).

39. B. A. S. Van Mooy, A. Rupke, S. T. Dyhrman, H. F. Fredricks, K. R. Frischkorn, J. E. Ossolinski, D. J. Repeta, M. Rouco, J. D. Seewald, S. P. Sylva, Major role of planktonic phosphate reduction in the marine phosphorous redox cycle. *Science* **348**, 783–785 (2015).

40. H. P. Hansen, F. Koroleff, in *Methods of Seawater Analysis*, K. Grasshoff, K. Kremling, M. Ehrhardt, Eds. (Wiley-VCH Verlag GmbH, Weinheim, Germany, 1999), pp. 159–228.

41. T. F. Thingstad, E. F. Skjoldal, R. A. Bohne, Phosphorus cycling and algal-bacterial competition in Sandsfjord, western Norway. *Mar. Ecol. Prog. Ser.* **99**, 239–259 (1993).

42. D. M. Karl, G. Tien, MAGIC: A sensitive and precise method for measuring dissolved phosphorus in aquatic environments. *Limnol. Oceanogr.* **37**, 105–116 (1992).

43. M. A. Charette, W. H. F. Smith, The volume of Earth's Ocean. *Oceanography* **23**, 112–114 (2010).